

AD-A115 149

PRINCETON UNIV NJ DEPT OF CHEMICAL ENGINEERING
PHOTOIONIZATION OF MOLECULAR CLUSTERS.(U)
DEC 81 R P ANDRES, J M CALO

F/G 7/4

UNCLASSIFIED

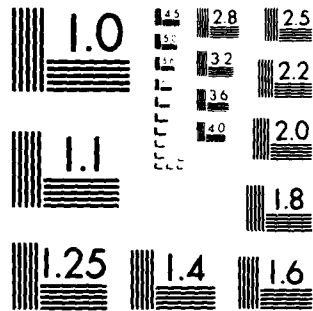
AFOSR-78-3638

AFOSR-TR-82-0451

NL



END
DATE
FILMED
7-82
DTIC



MICROCOPY RESOLUTION TEST CHART
NATIONAL BUREAU OF STANDARDS-1963-A

Unclassified
SECURITY CLASSIFICATION OF THIS PAGE (When Data Entered)

12

REPORT DOCUMENTATION PAGE		READ INSTRUCTIONS BEFORE COMPLETING FORM
1. REPORT NUMBER AFOUR-TR- 82-0451	2. GOVT ACCESSION NO. AD-A115149	3. REPORT'S CATALOG NUMBER
4. TITLE (and Subtitle) Photoionization of Molecular Clusters		5. TYPE OF REPORT & PERIOD COVERED Final Report
		6. PERFORMING ORG. REPORT NUMBER
7. AUTHOR(s) R.P. Andres and J.M. Calo		8. CONTRACT OR GRANT NUMBER(s) AFOSR-78-3638
9. PERFORMING ORGANIZATION NAME AND ADDRESS Department of Chemical Engineering Engineering Quadrangle, Princeton University		10. PROGRAM ELEMENT, PROJECT, TASK AREA & WORK UNIT NUMBERS 61102F 2303/B1
11. CONTROLLING OFFICE NAME AND ADDRESS AFOSR Directorate of Chemical Sciences (NC) olling AFB, Bldg. 410, Washington, D.C., 20332 MONITORING AGENCY NAME & ADDRESS (if different from Controlling Office)		12. REPORT DATE December 1981
		13. NUMBER OF PAGES 53
		15. SECURITY CLASS. (of this report) UNCLAS
		15a. DECLASSIFICATION/DOWNGRADING SCHEDULE

DISTRIBUTION STATEMENT (of this Report)

DISTRIBUTION STATEMENT (of the abstract entered in Block 20, if different from Report)

SUPPLEMENTARY NOTES

DTIC
ELECTRIC
JUN 04 1982
S E

19. KEY WORDS (Continue on reverse side if necessary and identify by block number) molecular clusters, photoionization, atmospheric nucleation, bipolar quadrupole mass spectrometry
20. ABSTRACT (Continue on reverse side if necessary and identify by block number) An experimental apparatus consisting of a novel multiple expansion cluster source coupled with a molecular beam system and photoionization mass spectro- meter has been designed and constructed. This apparatus has been thoroughly tested and preliminary measurements of the growth kinetics of water clusters and the photoionization cross section of the water dimer have been carried out.

DD FORM 1473 EDITION OF 1 NOV 65 IS OBSOLETE

Unclassified
SECURITY CLASSIFICATION OF THIS PAGE (When Data Entered)

82 06 04 013

DTIC FILE COPY . . . AD A115149

UNCLAS

PRINCETON UNIVERSITY
School of Engineering and Applied Science
Department of Chemical Engineering
Princeton, New Jersey 08544

"Photoionization of Molecular Clusters"

R. P. Andres and J. M. Calo

Final Technical Report

May 1, 1978 - September 30, 1981
For Grant No. AFOSR-78-3638

Submitted to

Air Force Office of Scientific Research
Directorate of Chemical Sciences (NC)
Bolling Air Force Base
Washington, D.C. 20332

Accession For	
NTIS GRA&I	<input checked="checked" type="checkbox"/>
DTIC TAB	<input type="checkbox"/>
Unannounced	<input type="checkbox"/>
Justification	
By	
Distribution/	
Availability Codes	
Dist	Avail and/or Special
A	



December 1981

Approved for
distribution

RESEARCH OBJECTIVES

Hydrated hydronium ions and other water-associated molecular cluster ions control the ion chemistry and possibly some of the neutral chemistry of the lower D region of the ionosphere. Similar cluster ions and neutral molecular cluster species have been proposed as nucleation initiators and precursors of aerosols and particulates in gas-to-particle conversion mechanisms in the stratosphere, and even in the troposphere. However, the formation and destruction mechanisms of these species and their chemical and physical properties are still not completely understood.

It has been theoretically predicted and experimentally observed, on a limited basis, that the ionization potential of a molecular cluster decreases with increasing cluster size and at some point becomes equal to that of the bulk phase. The existence of atmospheric cluster species and/or agglomerates of lower ionization potential than their molecular parents represents a potential low energy source of natural cluster ions. Experimental proof of this phenomenon would serve to elucidate, complement, amplify, and extend existing theories of atmospheric chemistry, nucleation, and gas-to-particle conversion.

A three year experimental research program has been pursued to construct and develop an atmospheric molecular cluster apparatus consisting of a novel multiple expansion cluster source (MECS) and a molecular beam sampling system with photoionization mass spectrometry detection and analysis. The use of this apparatus is directed at investigation and measurement:

1. Photoionization appearance potentials of water and water-associated molecular clusters;
2. The kinetics and rate constants for homogeneous homo- and hetero-molecular nucleation of atmospheric species; and

AIR FORCE OFFICE OF SCIENTIFIC RESEARCH (AFSC)
NOTICE OF TRANSMITTAL TO DTIC
This technical report has been reviewed and is
approved for public release IAW AFR 190-12.
Distribution is unlimited.
MATTHEW J. KERPER
Chief, Technical Information Division

3. The equilibrium mol fractions of homo- and heteromolecular dimers of atmospheric species.

STATUS OF RESEARCH EFFORT

Since the last Annual Technical Report dated June 1980 for AFOSR 78-3638 the entire photoionization apparatus including cluster source, molecular beam system, quadrupole mass spectrometer, VUV lamp, and VUV monochromator has been assembled and tested. Based on these tests the vacuum system was modified and a new set of electrostatic lens for ion focussing and a new quadrupole mass spectrometer were installed. The final experimental apparatus and its operating characteristics are summarized in Appendix A. A more detailed description of the VUV light source is included in Appendix B.

Preliminary measurements of the growth kinetics of homomolecular water clusters and the photoionization cross section of the water dimer have been carried out.

The following specific accomplishments have been realized:

1. Vacuum/Beam System

The vacuum system has been modified by eliminating the gate valve and the Varian HSA-2 diffusion pump which provided a close-off valve and differential pumping between the first vacuum chamber and the detection chamber respectively. Elimination of these elements: (1) shortens the distance photoionized clusters must travel before they are detected, (2) makes possible a greatly improved ion lens system, and (3) does not appreciably affect the vacuum in the detection chamber. The vacuum performance of the entire apparatus with the new gas load due to the hydrogen discharge VUV lamp is well within design specifications.

2. Mass Spectrometer

The mass spectrometer ion detection system described in the last Annual Technical Report dated June 1980 has been changed substantially. In order to increase the resolution, transmission, and stability of the mass filter, an Extranuclear mass spectrometer has been substituted for the EAI mass spectrometer. An ionizer and ion lens system has been built that: (1) permits both electron impact ionization and photoionization in a single ionization region located in the first vacuum chamber and (2) focuses ~50% of the cluster ions formed in the ionization region onto the entrance aperture of the quadrupole mass filter.

3. Signal Processing

The signal processing system has been improved so that phase-sensitive analog or pulse counting detection of the cluster ions is possible. The x-axis of the tracor Northern multichannel analyzer can now be synchronized with either the mass setting on the mass filter or the wavelength setting on the monochromator.

4. Water Cluster Source

Substantial operating experience has been achieved with the multiple expansion water cluster source. Several modifications of the design described in the last Annual Technical Report have been made. These changes are designed to control icing and temperature in the condensation region. A theoretical analysis of growth kinetics in a MECS for the conditions of the present research has been performed. The analysis, which is outlined in Appendix C, enables inversion of cluster ion intensity data to yield absolute rate constants for cluster growth.

5. VUV Light Source

A Hinteregger type gas discharge VUV light source has been built and tested. The design of this source and its operating characteristics are detailed in Appendix B. In conjunction with the 0.2 m monochromator, this source is capable of producing $\sim 10^{10}$ photons/sec at Lyman-alpha with a $\sim 5\text{\AA}$ bandwidth.

6. Photoionization Experiments

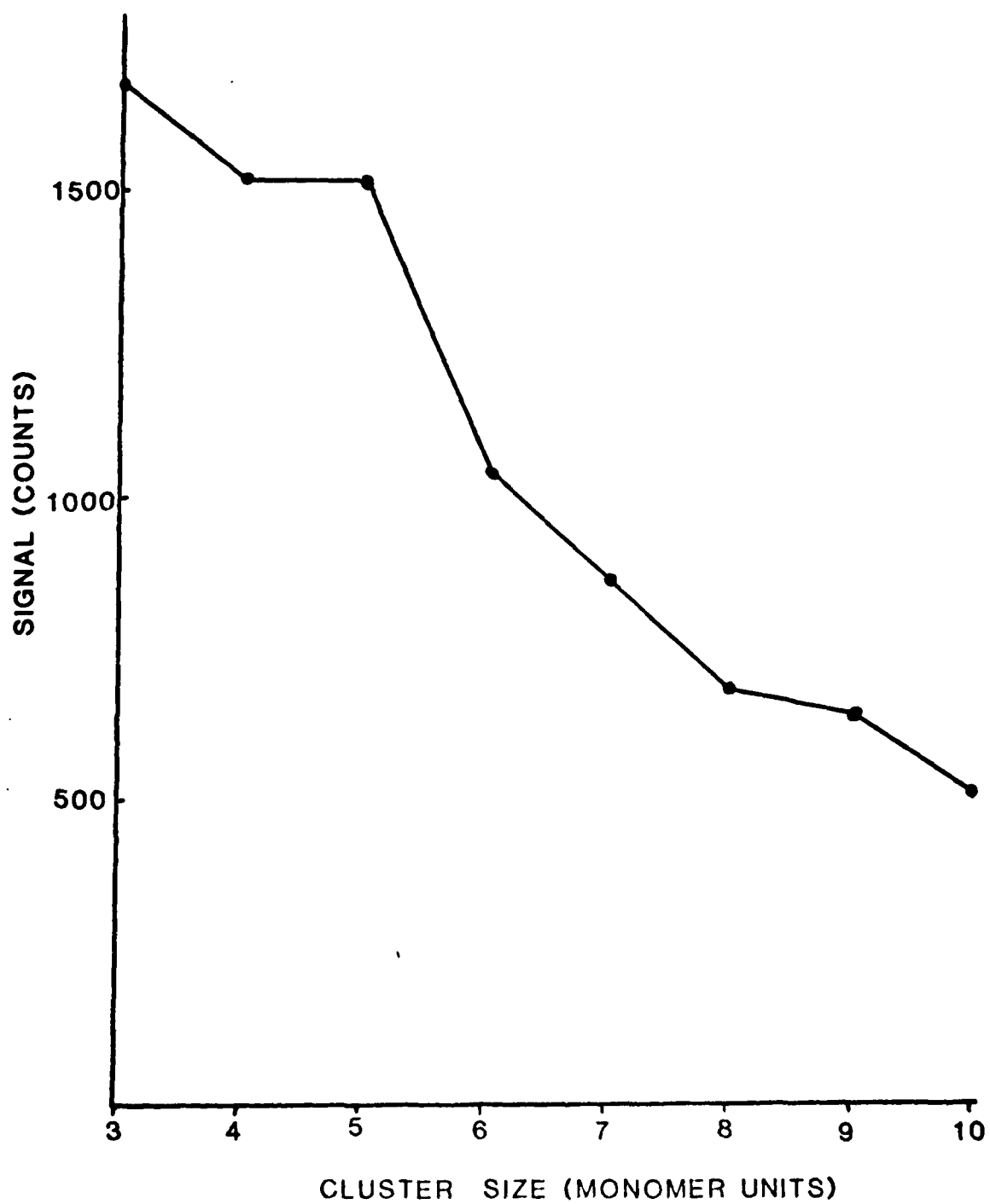
Photoionization experiments have been carried out on water monomer and water dimer. These experiments used an adiabatic free jet source in place of the MECS. The data reproduce those of earlier investigators (C.Y. Ng, D.J. Trevor, P.W. Tiedemann, S.T. Ceyer, P.L. Kronebusch, B.H. Mahan, and Y.T. Lee, J. Chem. Phys. 67, 4235, 1977).

The photoionization system works well and should be capable of measuring the desired photoionization cross sections of water clusters larger than the dimer if approximately 20 times the present photon intensity can be achieved.

7. Kinetic Experiments

Preliminary experiments have been carried out employing electron impact ionization of water clusters produced in the MECS. These experiments appear very promising. Figure 1 shows sample data from such an experiment. The inversion procedure outlined in Appendix C has been developed. It appears as though it will be possible to obtain accurate rate constants for water cluster growth. These rate constants have never before been measured.

CLUSTER ION SIGNAL vs. CLUSTER SIZE



CUMMULATIVE PUBLICATIONS

"Free Jet Deceleration - A Scheme for Separating Gas Species of Disparate Mass", N.K. Thuan and R.P. Andres, in Rarefied Gas Dynamics, Eleventh Symposium, Vol.1 (Campargue, Ed.), 667 Commissariat a l'Energie Atomique (1979).

"van der Waals Molecules - Possible Roles in the Atmosphere", J.M. Calo and R.S. Narcisi, Geophys. Res. Lett., 7, 289 (1980).

"Fokker - Planck Description of the Free Jet Deceleration Flow", T.K. Nguyen and R.P. Andres, in Rarefied Gas Dynamics, Progress in Astronautics and Aeronautics, 74: Part 1, (Fisher, Ed), 627 (1981).

"Generation of Molecular Clusters of Controlled Size", R.S. Bowles, J.J. Kolstad, J.M. Calo, and R.P. Andres, Surface Science, 106, 117 (1981).

"Melting Temperature of Small Particles", J. Ross and R.P. Andres, Surface Science, 106, 11 (1981)

PROFESSIONAL PERSONNEL

The following personnel were associated with the research effort:

Ronald P. Andres, Ph.D.
Professor
Department of Chemical Engineering
Princeton University

Joseph M. Calo, Ph.D.
Assistant Professor
Department of Chemical Engineering
Princeton University

Gerald F. Ryan, B.S.
Research Engineer
Department of Chemical Engineering
Princeton University

Jeffrey J. Kolstad, A.M.
Graduate Student
Department of Chemical Engineering
Princeton University

CUMMULATIVE PRESENTATIONS

J.J. Kolstad, J.M. Calo, and R.P. Andres,

"Generation and Photoionization of Molecular Clusters of Atmospheric Interest", Symposium on Atmospheric Aerosols, 178th National Meeting - ACS, Washington, D.C., September 11, 1979.

J.M. Calo and R.S. Narcisi,

"van der Waals Molecules - Possible Roles in the Atmosphere", VI International Conference on Atmospheric Electricity, UMIST, Manchester, England, July 28, 1980.

J.J. Kolstad, J.M. Calo, and R.P. Andres,

"The Generation and Photoionization of Molecular Clusters of Atmospheric Interest", VI International Conference on Atmospheric Electricity, UMIST, Manchester, England, July 28, 1980.

T.K. Nguyen and R.P. Andres,

"Fokker-Planck Description of the Free Jet Deceleration Flow:", Twelfth International Symposium on Rarefied Gas Dynamics, Charlottesville, July 10, 1980.

R.S. Bowles, J.J. Kolstad, J.M. Calo, and R.P. Andres,

"Generation of Molecular Clusters of Controlled Size", Second International Meeting on Small Particles and Inorganic Clusters", Lausanne, Switzerland, September 9, 1980.

J. Ross and R.P. Andres,

"Melting Temperature of Small Particles", Second International Meeting on Small Particles and Inorganic Clusters", Lausanne, Switzerland, September 9, 1980.

APPENDIX A

Atmospheric Molecular Cluster Apparatus

The cluster beam-photoionization mass spectrometer system which was developed for this research consists of four main elements:

1. vacuum system
2. cluster generator
3. cluster ionizer
4. mass spectrometer detector

Each of these elements is described below.

I. Vacuum System

The entire apparatus is schematized in Figure 1A. The vacuum system consists of three separately pumped chambers. The first chamber contains the cluster beam source and the ionization region. A GCA/McPherson (0.2m, f/4.5) monochromator forms the second chamber. The third chamber contains the mass spectrometer and electron multiplier detector.

The first chamber, which is fabricated out of aluminum, is designed to provide large pumping speed and to minimize the distance between the exit slits of the monochromator and the axis of the cluster beam. This chamber is pumped by a Varian VHS-6" oil diffusion pump with extended cold cap. Inside the chamber is a liquid nitrogen reservoir which supplies cooling to the cluster generator and serves as a cryopump for condensables.

The monochromator is pumped by a VHS-4" oil diffusion pump with a CVC liquid nitrogen cooled cryobaffle.

The third chamber is constructed from a stainless steel 6" cross and a half nipple. The cross is modified by addition of three small feedthrough ports. This chamber is pumped by a VHS-4" oil diffusion pump equipped with a gate valve and a liquid nitrogen cooled cryobaffle.

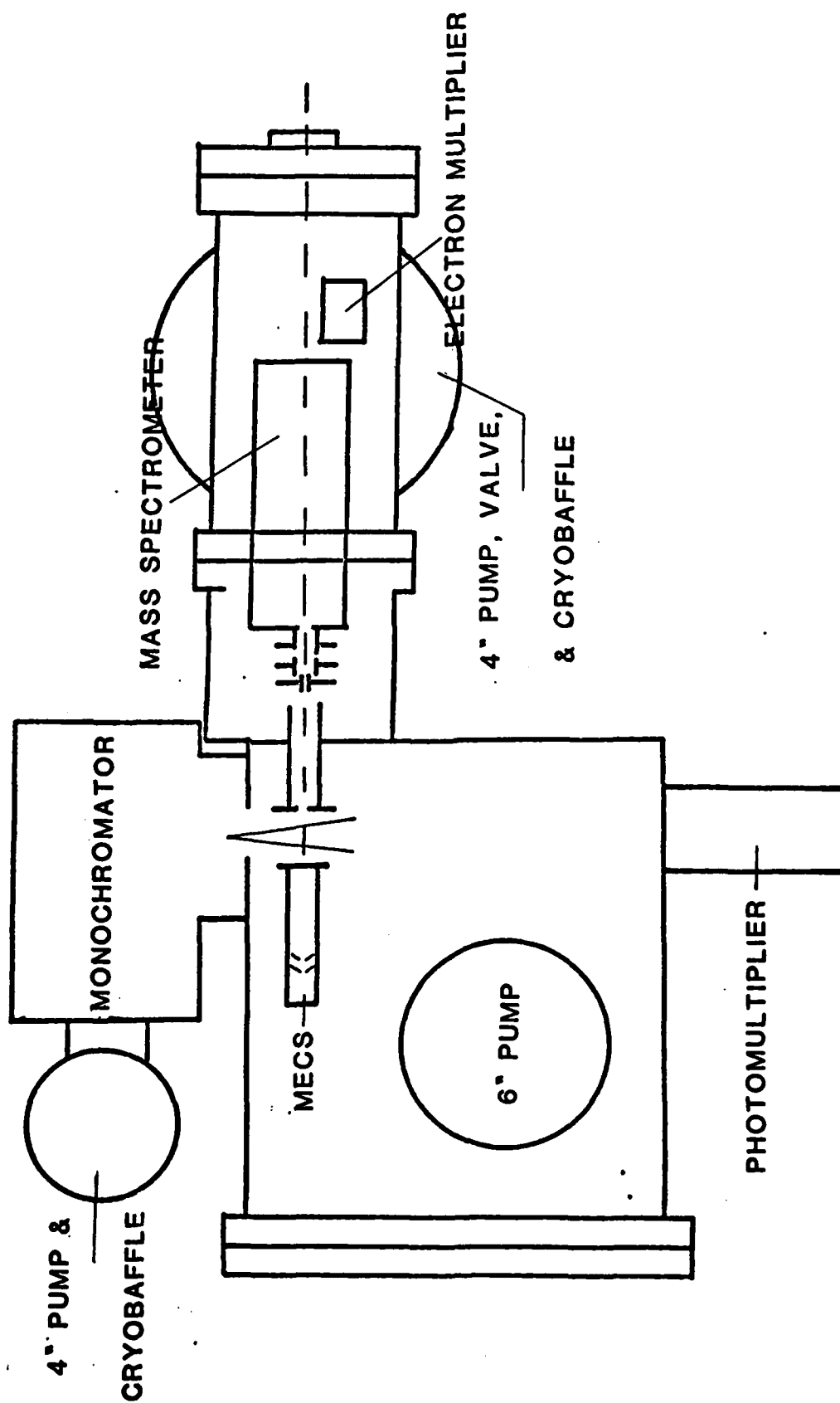


Figure 1A

ATMOSPHERIC MOLECULAR CLUSTER APPARATUS

All three oil diffusion pumps are backed by a single Leybold-Heraeus 12.5 l/s rotary vane pump. The pressures in all of the chambers can be monitored by means of Bayard-Alpert type ionization gauges and a Granville-Phillips 271-004 ion gauge controller, which also provides over-pressure protection to the VUV lamp and the detection electronics.

Typical operating pressures are 1×10^{-4} torr in the first chamber (the base pressure in this chamber is $\sim 1 \times 10^{-6}$ torr), 8×10^{-5} torr in the monochromator, and 5×10^{-6} torr in the detection chamber (the base pressure in this chamber is $\sim 1 \times 10^{-7}$ torr).

II. Cluster Generator

The standard method of generating small molecular clusters is by adiabatic expansion of a condensable vapor through a sonic orifice or nozzle into a vacuum. Adiabatic expansion produces a dramatic cooling of the gas while also lowering its density. The rapid cooling supersaturates the gas and results in cluster growth. This growth process stops when the gas density drops to the point where collisions between molecules of the condensable species become infrequent. The nozzle flow rate, hence the total number of collisions which can lead to growth, is limited by the pumping speed of the vacuum system. Since the gas temperature and density drop sharply during the expansion, control of cluster size and temperature are extremely difficult.

A novel method of producing small molecular clusters which overcomes many of these difficulties has been developed in the Beam Kinetics Laboratory at Princeton.^(1,2) This method has been termed the Multiple Expansion Cluster Source (MECS). The first MECS was designed to produce metal clusters. The MECS constructed for the Atmospheric Molecular Cluster Apparatus is similar to this metal cluster source, but it is designed to operate at cryogenic temperatures.

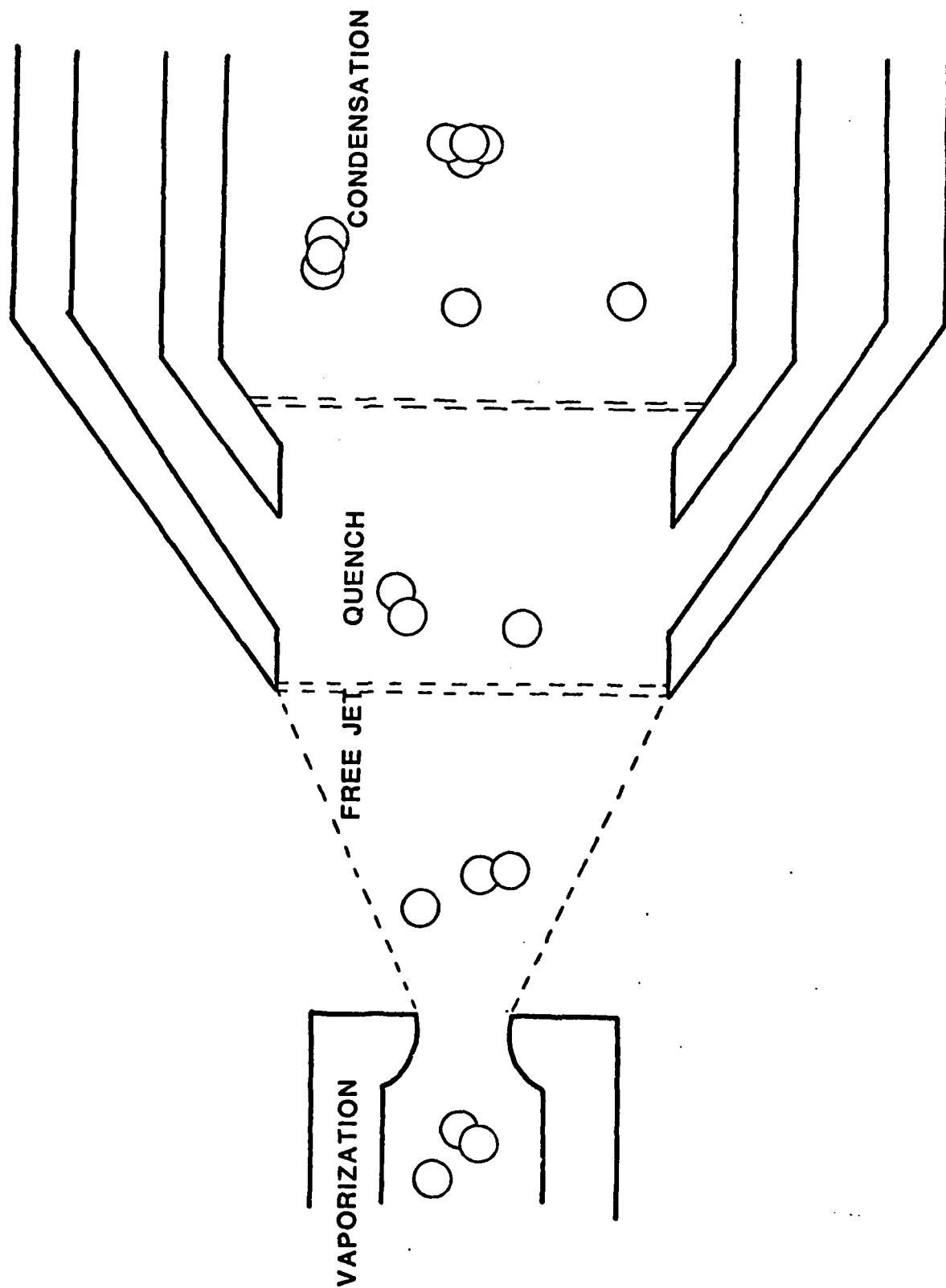
The MECS has substantial advantages over a supersonic free jet source. First, pressure and temperature can be varied independently; they are not constrained to lie along the path of an adiabatic expansion. Also, temperature is essentially constant during the growth process and, since growth occurs in a region of relatively high carrier gas density, the clusters are much closer to thermal equilibrium than they are in a free jet expansion. Although there is a small pressure drop down the length of the growth region and some of the condensable gas is lost to the wall of the growth region, the density of condensable species in a MECS remains nearly constant during cluster growth. The MECS can be thought of as an isothermal, fast flow reactor. Another attractive feature of this type of source is that with it one can approach "pure birth" kinetics, which result in the tightest distribution of cluster sizes possible in a condensation type source.

The schematic diagram below (Figure 2A) shows the essential parts of a multiple expansion cluster source. The first stage is the vaporization region where equilibrium is established between monomers and dimers of the condensable species and an inert carrier gas. The dimers present in this region serve later as "seeds" from which clusters grow.

The second stage is a supersonic free jet expansion, terminating in a normal shock. The partial pressure of the condensable species in this expansion is low enough so that essentially no cluster growth occurs here. The short residence time and the rapid cooling which characterize this expansion preserve the distribution of monomers and dimers established in the first stage. The normal shock defines the start of the quench zone and serves to isolate this region from the vaporization region.

MULTIPLE EXPANSION CLUSTER SOURCE

Figure 2A



The quench region is a zone of intense mixing and rapid supersaturation in which cold quench gas is added to the flow. The quench region is bounded on the upstream side by the first shock and downstream by a second shock which terminates a second supersonic free jet expansion into the condensation region. These shocks serve to confine the quench region to a very small volume and isolate it from the vaporization region and the condensation region. Negligible cluster growth occurs in the quench zone due to the short residence time here.

Cluster growth occurs in the condensation region by monomer addition onto clusters of two or more molecules. The growth kinetics are essentially irreversible if the supersaturation is high enough. Thus, pure birth kinetics are observed. Cluster growth occurs both on the dimers which formed in the vaporization region and on any new dimers which form in the condensation region. Cluster-cluster agglomeration is usually negligible as the monomer concentration greatly exceeds the total cluster concentration. The condensation region is essentially isothermal. As only the centerline is sampled, loss of condensate to the walls can often be neglected. Growth kinetics are easily studied in this region by varying the residence time. This is usually done by throttling the pump which evacuates the MECS. It could also be done by designing a MECS which has a variable length condensation zone. The clusters flow through a sharp edged orifice passing into the first vacuum chamber to form a molecular beam.

In summary the essential features of the MECS are: 1. a well defined, almost instantaneous, supersaturation and 2. subsequent cluster growth in an isothermal, fast flow, reactor. These features facilitate control over cluster temperature and size and simplify study of cluster growth kinetics.

Figure 3A gives relevant construction details of the MECS used to grow water clusters. The vaporization region consists of a 1/8" pyrex tube, which is necked down at the end to form a converging nozzle. Several different size nozzles are used having flow rates ranging from 3 to 15 cm³/sec at STP. Each nozzle tube is epoxied into a 1/4" diameter brass rod and this assembly is sealed by means of a modified Cajon Ultra-Torr fitting to a brass nozzle holder. The nozzle holder is heated electrically. The temperature and the pressure in the pyrex tube and in the region surrounding the nozzle are both monitored.

The first skimmer (0.080" aperture) is machined from copper and is soldered into the end of the nozzle holder. It is heated by conduction. The second skimmer (0.090" aperture) is also machined from copper and is force fit into the condensation zone mount. A nylon gasket separates the nozzle holder from the condensation zone mount. Its purpose is to thermally isolate those two pieces while maintaining a vacuum seal. A location ring is machined in this gasket to insure good alignment between the two skimmers which define the quench region.

The copper tube which serves as the condensation zone is cooled by conduction through its mount, which is machined from copper, and through a 7/16" copper rod soldered to the mount. This rod is clamped to a liquid nitrogen reservoir. It serves as the mounting stem for the MECS. The condensation zone is approximately 6.5cm long with an I.D. of 1.0cm. The temperature and pressure in the condensation zone are measured with a digital thermometer and absolute pressure gauge.

The final skimmer, which defines the fraction of the condensation zone flow which passes into the vacuum chamber to form a molecular beam, has a heater which can be used to prevent icing. This skimmer may be either flat or conical in shape. A 200 Hz Bulova tuning fork optical chopper is used to modulate the beam before it is ionized. In order to shorten the distance between the ionizer and the MECS, the final skimmer serves as the ionizer mount.

WATER CLUSTER SOURCE

Figure 3A

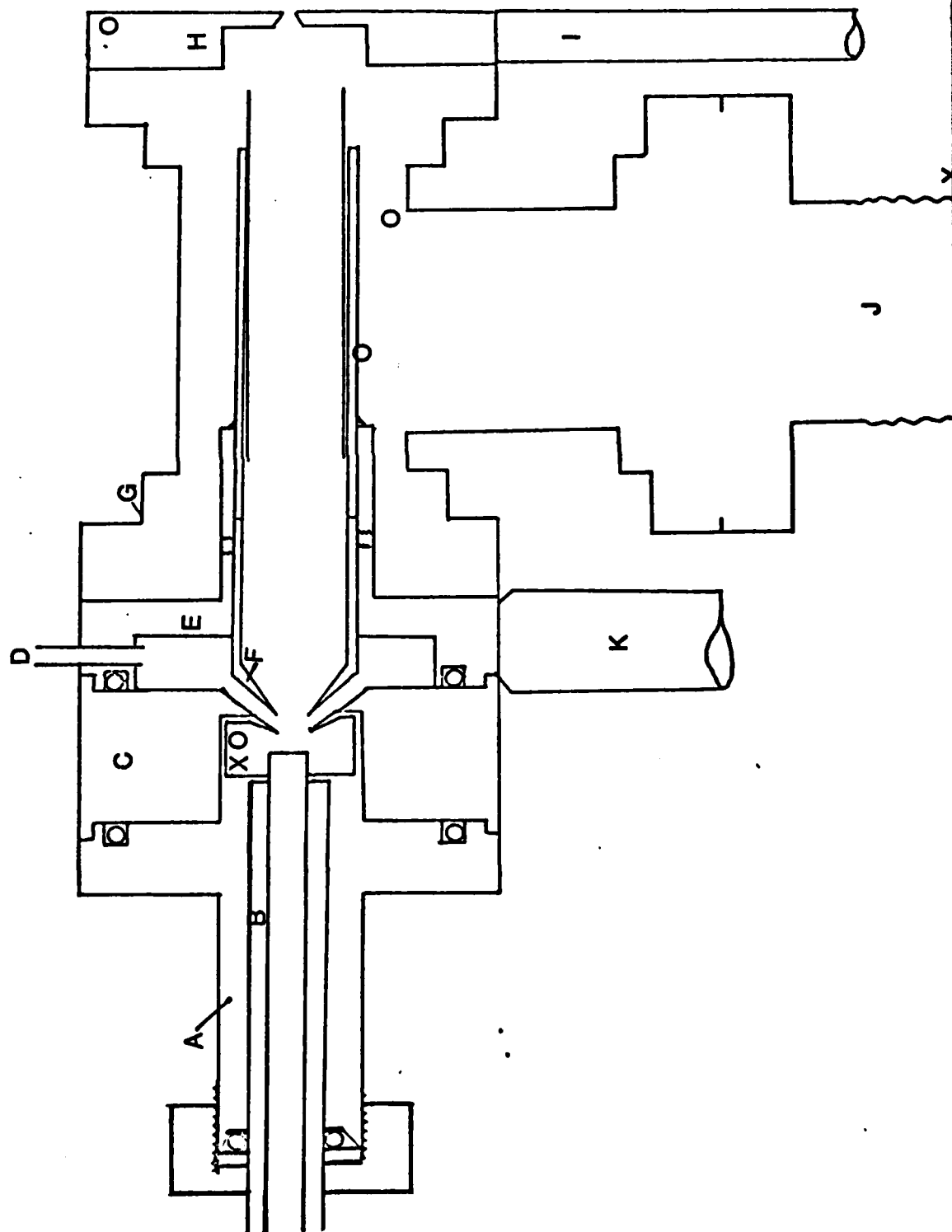


Figure Caption

- (A) Nozzle holder
- (B) Nozzle assembly
- (C) Nylon gasket
- (D) Quench gas inlet
- (E) Condensation zone mount
- (F) Condensation zone
- (G) Modified stainless steel tee
- (H) Final skimmer
- (I) Heating rod
- (J) To pump
- (K) Cooling rod

O - Thermocouple locations

X - Pressure taps

The condensation zone is pumped by a Leybold-Heraeus 12.51/s rotary vane pump. Condensation zone pressure is monitored with an MKS/Baratron meter while nozzle pressures are measured with a Wallace and Tiernan gauge. Temperatures are monitored with a Fluke 2166A digital thermometer. Type J thermocouples with 0.010" teflon coated wires are used. Typical operating condition of the MECS are given in Table 1^A.

Several experiments have been carried out to verify the operation of the MECS. The quench pressure increases only 1% when the condensation pressure is increased 50% by throttling the pump; the increase is <0.2% for a 25% change in downstream pressure. The pressure drop in the condensation zone is linear with distance and corresponds to approximately 10% of the mean pressure for the conditions in Table 1^A. A pressure tap downstream of the condensation region can be used to estimate the pressure in the condensation zone to within 2%, even while throttling the pump. Thus, the problem of disturbing the flow inside the condensation zone with a pressure tap can be avoided.

The effect of wall temperature on the centerline temperature in the condensation region is minimized by maintaining the wall and the gas mixing temperatures nearly equal. Since the conduction time from the wall of the flow in centerline of the flow is much longer than the residence time of the flow in the condensation region, the effect of wall temperature is slight even without this precaution.

TABLE 1A

Typical Operating Conditions for MECS

Nozzle	$T_o = 300-350^\circ\text{K}$ $P_o = 250 \text{ torr}$ $P_w = 5-50 \text{ torr}$ $d_n = 0.01 \text{ cm.}$
Free Jet	$l_j = 0.03 \text{ cm.}$ $t_j = 3 \times 10^{-7} \text{ sec.}$
Quench	$t_q = 80 \text{ K}$ $p_q = 9 \text{ torr}$ $d_q = 0.2 \text{ cm.}$ $l_q = 0.1 \text{ cm.}$ $t_q = 2 \times 10^{-6} \text{ sec.}$
Condensation	$T_c = 100 \text{ K}$ $P_c = 3 \text{ torr}$ $d_c = 1.0 \text{ cm.}$ $l_c = 6.0 \text{ cm.}$ $t_c = 2 \times 10^{-3} \text{ sec.}$

III. Cluster Ionizer

The ionizer is designed so that either electrons or photons can be used to ionize the clusters. Electron bombardment ionization has the advantage of producing higher cluster ion intensities, however, this technique cannot yield photoionization thresholds or photoionization cross sections

The VUV monochromator is operated without windows. The ionization potential of water monomer is 12.6 eV ($\sim 1000\text{\AA}$) which is too short a wavelength for transmission through any known window. Light of this wavelength has a low reflectivity on most surfaces and therefore is not readily focussed. Thus, it is important to locate the exit slits of the monochromator as close to the cluster beam axis as is possible to avoid intensity loss due to the divergence of the light beam. This distance is 4 cm. in the present apparatus. By locating the ionization volume close to the final skimmer of the MECS, the effects of cluster beam divergence are also minimized and the cluster ion signal is further increased.

Figure 4^A is a schematic diagram of the cluster ionizer. This figure shows the final skimmer of the MECS, the Bulova tuning fork chopper, the ion lens system that is used to focus the cluster ions, and the vacuum wall that separates the first chamber in which the neutral clusters are formed from the chamber in which the cluster ions are mass analyzed and detected.

Figure 4A

CLUSTER IONIZER

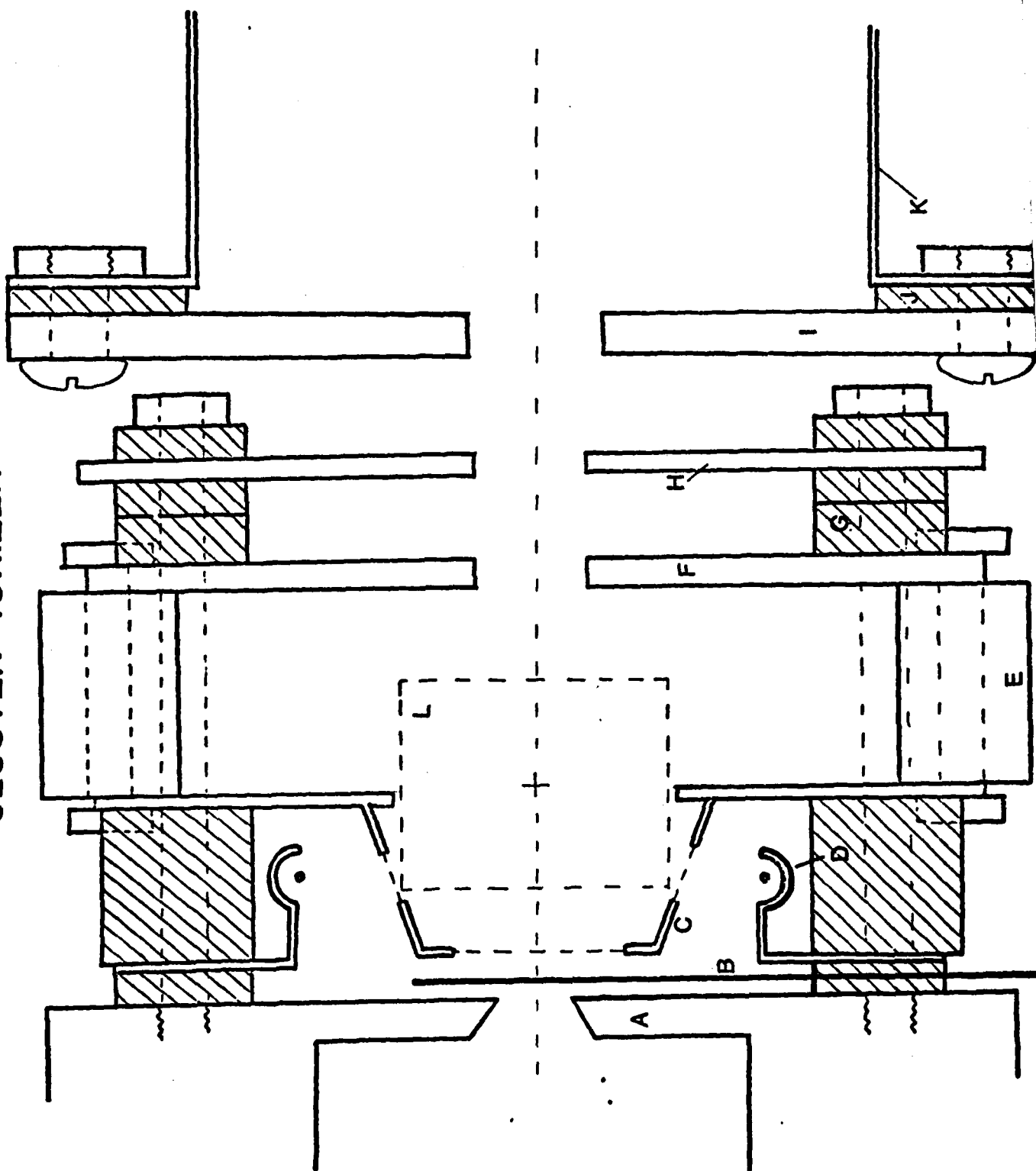


Figure Caption

- (A) Final skimmer of MECS
Orifice diameter, 0.020"
- (B) 200 hz Bulova tuning fork chopper
- (C) Ionization Region - Front plate and electron accelerator (stainless steel)
Front mesh opening (90% open), 17/64"
- (D) Filament Assembly
- (E) Spacer for extending ionization region, 5/16" long x 3/16" O.D. (brass)
- (F) Ionization Region - Back plate (stainless steel)
- (G) Insulating spacers (alumina)
- (H) Extraction plate 1 (stainless steel)
Opening 10/64"
- (I) Extraction plate 2 and vacuum wall (stainless steel)
Opening 3/16"
- (J) Insulating gasket (teflon, 1/32" thick)
- (K) Focussing tube, 4" long x 31/32" I.D. (stainless steel)
- (L) Cross section of VUV light beam

Operating voltages (typical)

- A,B ground
 - C,E,F, +15v
 - D -90V relative to C
 - H,I -180 V
 - K +6.5V (fine tune for preliminary focussing)
 - Lens 1 -50V
 - Lens 2 -30V (fine tune for focussing into quadrapole)
- } Mounted from mass spectrometer

The cluster ionizer is assembled using parts from a commercial dual filament axial beam ionizer (R.M. Jordan Co., Mountain View, CA), designed for the EAI quadrupole mass spectrometer. The ionization region was lengthened so that the same ionization volume and ion focusing lenses can be used for electron or photon ionization. Use of the identical ionization volume and ion focussing lenses in each case permits fine tuning of the focus with a relatively strong electron bombardment signal before switching over to photoionization.

The VUV monochromator and light source are discussed in detail in Appendix B.

IV. Mass Spectrometer Detector

The cluster ions are mass analyzed and detected by a quadrupole mass filter and an electron multiplier detector. Figure 5^A is a schematic drawing of the mass spectrometer, the off-axis multiplier, and the ion lens system which focuses the ions for transmission through the mass spectrometer.

An Extranuclear Model 270-9 quadrupole mass filter is used to mass analyze the cluster ions. Originally an EAI quadrupole mass filter was employed, but this instrument did not have adequate resolution or stability.

A Johnston Labs MMI, 20 stage, Cu-Be, electron multiplier is used for ion detection. High voltage to the multiplier is supplied by a Fluke 210B, $\pm 10,000$ volt power supply. The multiplier can be used either in a pulse counting or in an analog or total current mode. In the analog mode the multiplier signal is digitized by means of a Traycor-Northern NS-570A digital signal analyzer and stored as counts. In the pulse counting mode the multiplier output is fed to a Johnston Labs PAD-2 pulse amplifier-discriminator and the resulting counts are stored by the NS-570A. Since the cluster beam is modulated, the signal acquisition in both pulse and analog modes has been made phase sensitive.

The electron multiplier gain is about 10^4 at 2800 volts and exhibits a ten fold increase every 400 volts. A graph showing pulse counting rate as a function of discriminator level is shown in Figure 6^A. A rather broad distribution of pulse heights is indicated by this figure. Such a response is characteristic of Cu-Be multipliers at low ion energies ($< 3\text{kv}$).

DETECTION CHAMBER

Figure 5A

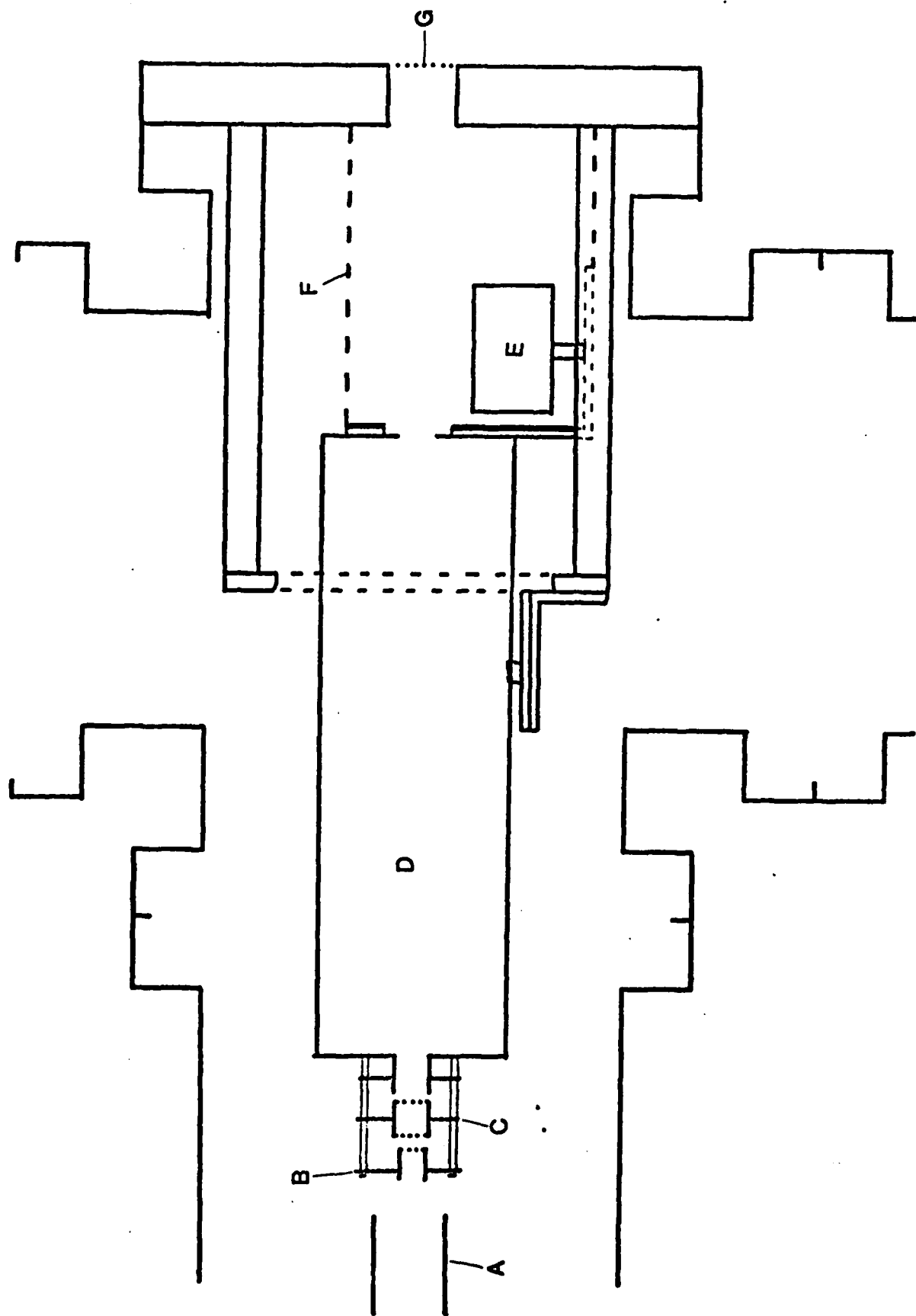


Figure Caption

- (A) Focussing tube
- (B) Lens 1
- (C) Lens 2
- (D) Quadrupole mass filter
- (E) Electron multiplier
- (F) Electrostatic shield
- (G) Viewing port

MULTIPLIER RESPONSE CURVE

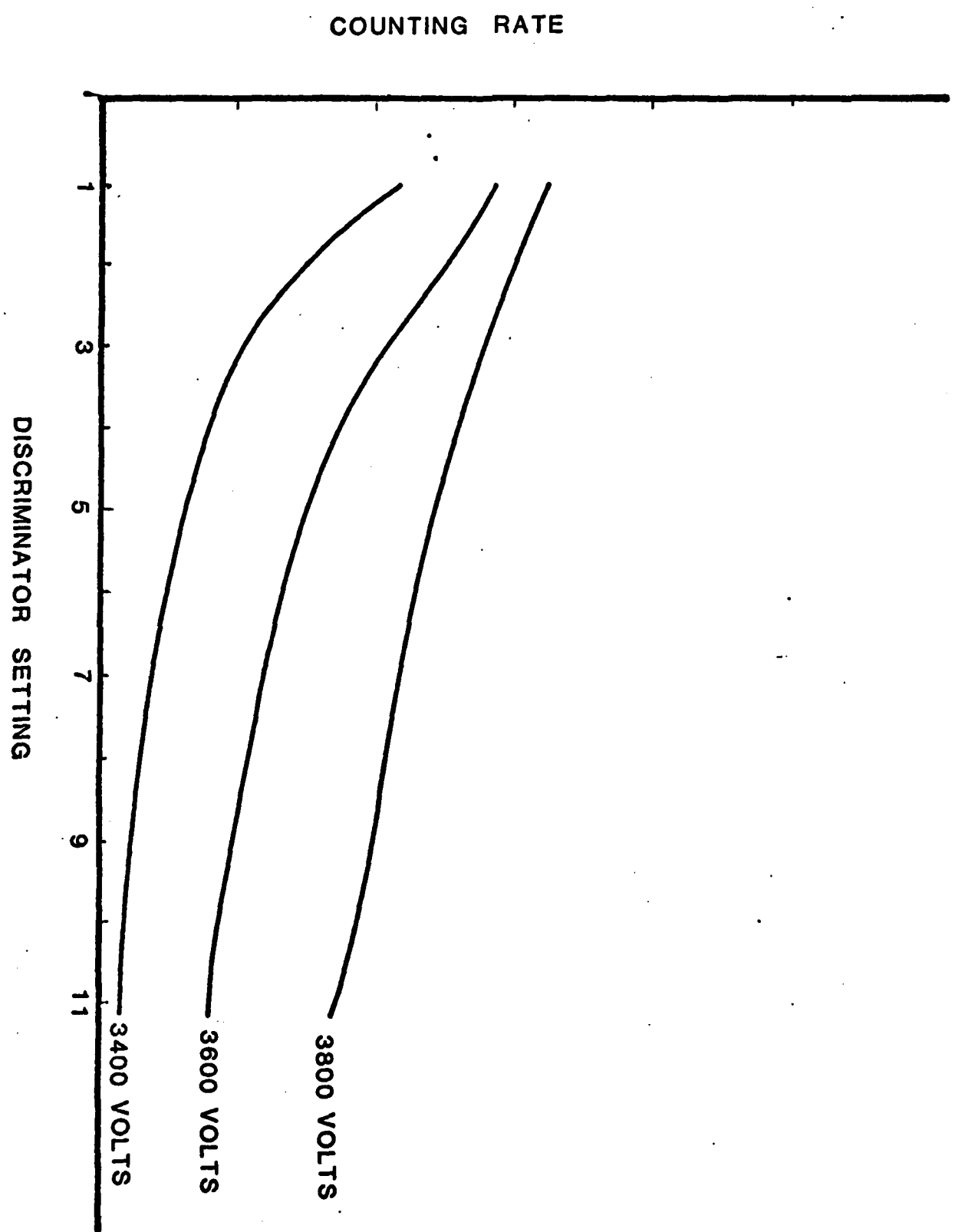


Figure 6A

A two element ion lens is used to collect and focus ions into the mass filter. The transmission of the entire ion lens system was determined by measuring total ion current on various lens elements as the voltage of the next element was raised to a repelling potential. Of the ions transmitted from the ionizer into the focussing tube (i.e., into the detection chamber) ~50% were transmitted through Lens 1 and ~10% were transmitted through the mass filter onto the first stage of the electron multiplier. Thus, approximately one out of every ten cluster ions that are extracted from the ionizer reach the electron multiplier.

- (1A) M. P. Taytelbaum, "Production of Monodispersed Copper Clusters from a Multiple Expansion Source", PhD. Thesis, Princeton Univ., 1977.
- (2A) G.L. Griffin, "Production of a Molecular Beam of Liquid-Free Metal Clusters", PhD. Thesis, Princeton Univ., 1979.

APPENDIX B

VUV Light Source

Equipment

The VUV light source developed for photoionization of cluster beam species, as described in Appendix A, essentially consists of a lamp, a monochromator, and a photomultiplier tube detector plus sundry supporting equipment.

The lamp as originally purchased was a GCA/McPherson model 630 vacuum ultraviolet Hinteregger cold cathode gas discharge lamp. This lamp operates with a water-cooled quartz capillary and anode, and a forced air convection-cooled cathode. For this project the lamp was modified by the addition of a hot tungsten filament as suggested in a published note by Eastman and Donelon (1B). It is claimed that "For practical operating conditions, this results in about a 10-fold intensity increase, four fold increase in time between cleanings, increased stability, and lower power supply cost" (1B). Schematics of the modification and power supply circuit are presented in Figure 1B. In our work the filament power was supplied via an AC autotransformer. An ammeter in the circuit monitored the filament current, which under typical operating conditions was 15A AC. The filament was made from approximately 10 cm of 0.015 in. diameter tungsten wire coiled twice around a 1/4" diameter cylinder such that the final configuration was 2 cm long by 1 cm in diameter (see Figure 1B). An Electronic Measurements SCR-EM 600/4 (600V, 4A), current-controlled power supply in series with a 50 ohm, 400w ballast resistor was used to initiate and maintain the discharge in the lamp. Under typical operating conditions the discharge required 1.5 A at voltages between 150 - 200 VDC.

The gas discharge lamp was mounted on the input port (entrance slit) of a GCA/McPherson model 234 (0.2m, f/4.5) vacuum ultraviolet scanning monochromator. The monochromator is equipped with a 1200 grove/mm corrected holographic concave reflectance grating, coated with Acton Research Corp. No. 1200 (Lyman- α) Al and MgF₂. This grating is blazed at 110 nm and has a reciprocal dispersion of 3.37nm/mm at 100 nm. The monochromator wavelength drive is connected to a stepping motor driven by a Superior Electric STM 103 translator and power supply. In the most recent configuration, the wavelength drive is controlled by the Tracor Northern digital signal analyzer with preset dwell times.

The output of the lamp/monochromator combination is monitored with a GCA/McPherson model 650 detector system consisting of an EMI 9635B photomultiplier tube (S-20 spectral response) with a vacuum-tight sodium salicylate converter window. Ultraviolet radiation impinging on the window causes the sodium salicylate to fluoresce which is then detected by the photomultiplier tube. The response of the sodium salicylate is uniform for wavelengths between 30 - 340 nm. The maximum in the sodium salicylate emission spectrum (\sim 443nm) is matched to that of the S-20 photomultiplier response (\sim 420 nm).

For assembly, testing and calibration purposes the entire VUV light source system was mounted on a separate test stand shown in Figure 2B (a-c). As shown, the monochromator is pumped by a Varian VHS-4, 4" diffusion pump with a Mexican hat cold cap, backed by a Sargent-Welch DUO-SEAL model 1402, two stage rotary vane mechanical vacuum pump. The diffusion pump is trapped with a liquid nitrogen-cooled baffle. The configuration shown in Figure 2B (a-c) is essentially the same as when mounted on the Atmospheric Molecular Cluster Apparatus, as described in Appendix A. The only differences are that the monochromator output port is mated to the first stage of the

apparatus instead of the photomultiplier detector, and the latter is mounted on a directly opposed opening on the other side of the first stage, as shown in Figure 1A.

System Operation and Performance

For the current work with water and water clusters, the continuum and line spectrum of hydrogen was found to be the most suitable, both from wavelength and intensity considerations. Figure 3B is a typical spectrum obtained with Matheson ultra-high purity hydrogen in the lamp and the photomultiplier detector mounted directly on the monochromator exit port. (See the figure caption for a summary of the experimental conditions.) During the early part of 1981 this grating was sent back to Acton Research Corporation for resurfacing. The resurfaced grating exhibited approximately a factor of four improvement in intensity at 122 and 159.8 nm, and about 1.4 at 486 nm.

Due to the relatively high breakdown potential of hydrogen, the lamp was usually started with pure argon or argon-hydrogen mixtures. A typical spectrum obtained using pure argon (Matheson, prepurified) at a lamp pressure of 0.055 torr is presented in Figure 4B for comparison. The intensities in the low wavelength region are obviously considerably lower than with hydrogen at 0.1 torr although emission at the higher wavelengths is comparable. Subsequent to the establishment of the discharge with argon, the gas in the lamp is gradually changed over to pure hydrogen. A detailed operating procedure, developed after considerable operating experience, is presented in Attachment 1B. This procedure results in stable, reproducible operating conditions and a filament lifetime of 4-6 hours in continuous operation, which although somewhat short, is not inconveniently so.

The output of the lamp/monochromator combination was measured on the test stand using the NO ionization chamber schematized in Figure 5B, modeled after those of Samson (2B) and Matsuoka and Oshio (3B). Essentially, the known photoionization characteristics of NO in an ion chamber designed to insure collection of all the ions produced was used to calibrate the lamp/monochromator output. A typical ion current output spectrum is presented in Figure 6B for 2.04 torr of NO in the ionization chamber and the discharge lamp conditions indicated.

The incident photon intensity corresponding to the collected ion current in the ionization chamber is determined as follows. At 122 nm the photoionization yield of NO is reported to be, $Y = 0.81$ (Watanabe et. al., (4B)). At 122 nm, the collected ion current, $i_{ion} = 27.1$ nA. Therefore,

$$Y = 0.81 = \frac{i_{ion}}{I_{abs}}$$

where I_{abs} is the photon intensity absorbed in the ionization chamber.

$$I_{abs} = \frac{i_{ion}}{0.81} = \frac{2.71 \times 10^{-8} \text{ A}}{1.6 \times 10^{-19} \frac{\text{coul}}{\text{ion}} \frac{\text{A}}{\text{coul/s}}} (0.81)$$

$$I_{abs} = 2.09 \times 10^{11} \text{ photons absorbed}$$

Also, $I_0 - I_{trans.} = I_{abs}$

From the Beer-Lambert law:

$$\frac{I_{trans}}{I_0} = \exp(-kx)$$

where k is the absorption coefficient, or macroscopic cross section and x is the absorption path length. From Watanabe et. al. (4B) $k = 65.4 \text{ cm}^{-1}$, and correcting for pressure and temperature:

$$k = 65.4 \text{ cm}^{-1} \left(\frac{2.04}{760} \right) \left(\frac{273.15}{292} \right) = 0.1642 \text{ cm}^{-1}$$

$$\frac{I_{\text{trans}}}{I_0} = \exp(-0.1642 \text{ cm}^{-1} \times 10 \text{ cm})$$

$$= 0.194$$

$$1 - \frac{I_{\text{trans}}}{I_0} = \frac{I_{\text{abs}}}{I_0} = .806$$

Finally, allowing for the transmittance of the MgF_2 window on the ionization chamber (measured as ~83.5% at 122nm):

$$I_0 = \frac{I_{\text{abs}}}{(.806)(0.835)} = \frac{2.09 \times 10^{11}}{(.806)(0.835)}$$

$$I_0 = 3.10 \times 10^{11} \text{ photons/s}$$

The spectral bandwidth (SBW) is given by the product of the physical slit width and the linear dispersion function of the monochromator:

$$\text{SBW} = 2.0 \text{ mm} \times 3.37 \text{ nm/mm} = 6.74 \text{ nm}$$

Therefore, the total specific output at 122nm is 4.6×10^{10} photons/s-nm. With the resurfaced grating used in the current system, this value becomes $4.6 \times 10^{10} \times 4.42 = 2.0 \times 10^{11}$ photons/s-nm. Also, because there is no window between the lamp and the monochromator, the entrance slit was stopped down to 0.2 mm due to pumping speed constraints. Since the transmitted intensity is proportional to the entrance and exit slit widths, with a 2 mm entrance slit, the equivalent intensity output becomes 2.0×10^{12} photons/s-nm, which is quite comparable to the 1.625×10^{12} photons/s-nm quoted by Eastman and Donelon (1B).

Studies with the ionization chamber also revealed the presence of higher order reflections in the spectrum caused by overlapping orders from the grating; e.g., radiation output at 240 nm also includes a 120 nm component.

This results in an incomplete cut-off of ionization thresholds greater than 120 nm unless a filter (e.g., LiF) is used to eliminate the high energy photons. At wavelengths below 120 nm a filter is not required since the lamp output below 60 nm is negligible.

References

- (1B). Eastman, D. E. and J. J. Donelon, Rev. Sci. Instrum. 41, 1648 (1979).
- (25). Samson, J. A. R., J. Opt. Soc. Am. 54, 6 (1964).
- (3B). Matsuoka, T. and T. Oshio, Rev. Sci. Instrum. 45, 1012 (1974).
- (4B). Watanabe, K., F. M. Matsunaga, and H. Sakai, App. Opt. 6, 391 (1967).

Attachment 1B

Operating Procedures for Modified Hinteregger VUV DC Discharge Lamp

A. Start-Up

1. Set plunger control on monochromator entrance (lamp) slit to "0", and open slit to 2000 μm (2.0 mm). Open monochromator exit slit to 2000 μm (2.0 mm).
2. Turn on mechanical vacuum pumps and reduce the pressure in the lamp to approximately 10 mtorr (thermocouple gauge #1).
3. Add 5 liters of liquid nitrogen to the reservoir. At 10^{-5} - 10^{-6} torr the cryotrap will use about 1 liter of liquid nitrogen per hour.)
4. Close the lamp slit down to 50 μm and set plunger on "C".
5. Turn on the cooling water for the lamp and the diffusion pump (same line) at approximately 1.5 ℓ/min .
6. Plug in 120 VAC leads to the relay board on the lamp table.
7. Turn on the diffusion pump. Wait about 15 minutes and turn on ionization gauge.
8. The pressure in the monochromator must be below 5×10^{-5} torr before gas can be introduced into the lamp.
9. Pressurize the lamp with ~ 0.1 torr of argon. Thermocouple gauge #1 is used to measure the pressure in the lamp.
10. Bleed in an additional ~ 0.1 torr of hydrogen. The monochromator pressure should now be between 2×10^{-4} and 9×10^{-5} torr.

11. When the monochromator pressure is in the 10^{-5} range, the lamp can be started.
12. Turn on the 600V DC power supply to 600V and set the current control below 2A. to hold when the lamp is ignited. Plug in the powerstat connected to the filament autotransformer and the AC ammeter.
13. Turn up the powerstat slowly and the lamp should ignite between 10A and 15A AC. Set the lamp filament current to 15A AC.
14. Turn down the DC discharge current on the 600V DC power supply to 1.5A DC. The DC discharge voltage should then be between 150V and 200 V DC.
15. Turn off the argon supply. The lamp pressure should decrease to 0.1 torr hydrogen (on thermocouple gauge #1).
16. Increase the hydrogen lamp pressure to 0.2 torr and open the lamp slit to 200 μm . This should cause the hydrogen lamp pressure to fall to approximately 0.1 torr. Adjust the fine metering valve in the hydrogen line to maintain exactly 0.1 torr hydrogen in the lamp.
17. Check the metal thermometer located in the lamp housing. The temperature should be about 60°C .

18. Summary

Starting Conditions:

$P_{\text{H}_2} = 0.1 \text{ torr}$

$P_{\text{Ar}} = 0.1 \text{ torr}$

Lamp slit = 50 μm

Exit slit = 2000 μm

Running Conditions:

$P_{H_2} = 0.1 \text{ torr}$

Lamp slit = 200 μm

Exit slit = 2000 μm

$P(\text{monochromator}) = 5 \times 10^{-5} \text{ torr}$

$P(\text{manifold}) = 20 \text{ m torr}$

$T(\text{lamp}) = 60^\circ\text{C}$

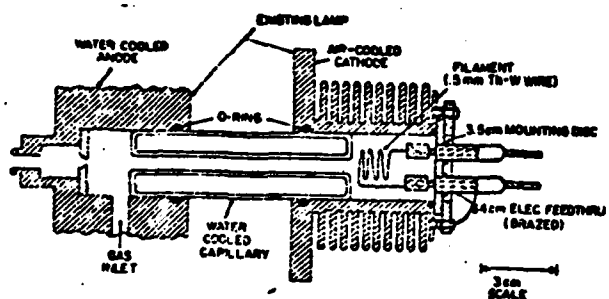
$I(\text{filament}) = 15\text{A AC}$

$I(\text{discharge}) = 1.5 \text{ A DC}$

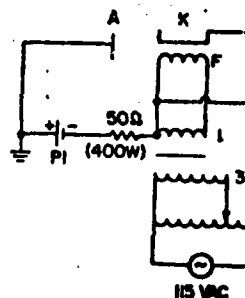
$V(\text{discharge}) = 180 \text{ V DC}$

B. Shut-Down

1. Turn the 600 V DC power supply off.
2. Turn off the hydrogen flow.
3. When the lamp pressure decreases to about 10 mtorr, turn off the AC filament current.
4. Turn off diffusion pump.
5. Turn off the lamp housing fan.



Physical lamp modification for hot filament operation. The filament assembly is shown with heavy lines.



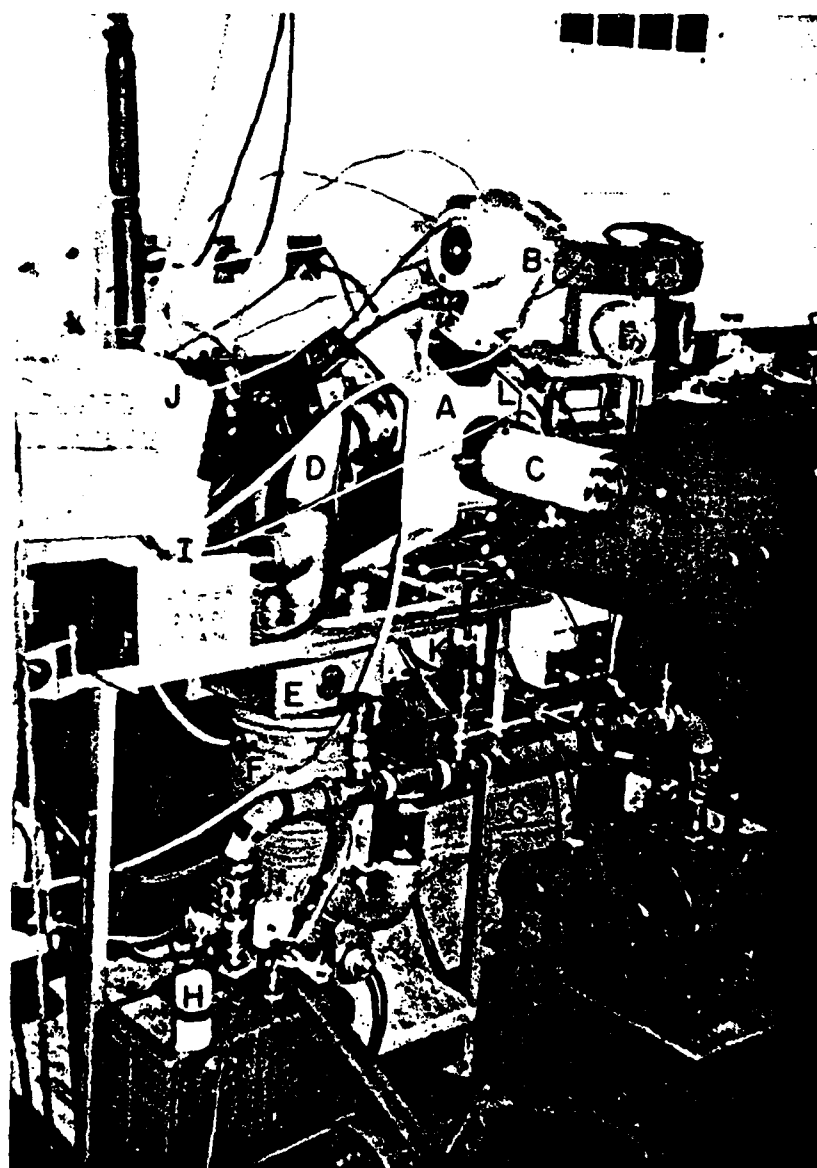
Schematic power supply circuit for hot filament operation. P1 is a current regulated 600 V, 2.5 A supply.

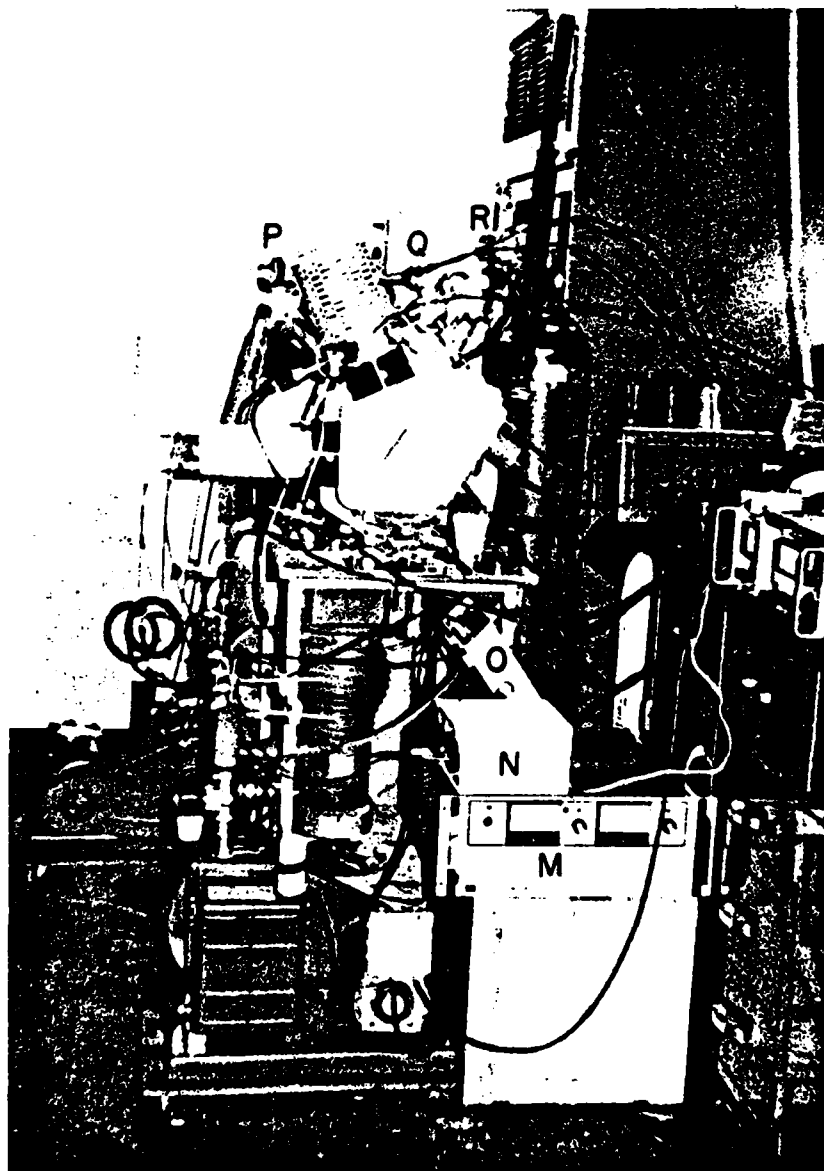
Figure 1B. Hot filament modification and power supply circuit for the Hinteregger VUV DC discharge lamp (from Eastman and Donelon (1B)).

Figure 2B. VUV light source apparatus: (a) front view; (b) side view; and (c) laboratory bench view.

Legend

- (A) VUV monochromator
- (B) VUV Hinteregger discharge lamp
- (C) Photomultiplier detector
- (D) 90° stainless steel elbow
- (E) Liquid nitrogen trap
- (F) 4" diffusion pump
- (G) Mechanical vacuum pump (2.67 ℓ /s)
- (H) Mechanical vacuum pump (2.67 ℓ /s)
- (I) Ionization gauge tube (10^{-4} - 10^{-10} torr)
- (J) Liquid nitrogen reservoir to feed trap (E)
- (K) Thermocouple gauge tube (1-1000 m torr)
- (L) Thermocouple gauge tube (1-1000 m torr)
- (M) Discharge lamp power supply (600 V, 4A)
- (N) Photomultiplier high voltage power supply.
- (O) Digital picoammeter for photomultiplier output and NO ionization chamber (10^{-9} to 10^{-3} A)
- (P) NO gas cylinder for ionization chamber (Matheson, C. P.)
- (Q) H₂ gas cylinder for discharge lamp (Matheson, ultrahigh purity)
- (R) Ar gas cylinder for initiating gas discharge (Matheson, prepurified)
- (S) Thermocouple/Ionization gauge controllers
- (T) Discharge lamp tungsten filament AC transformer (variable auto-transformer) and ammeter for current control.
- (U) Polyfoam-insulated phenolic laminate vent pipe for liquid nitrogen trap.





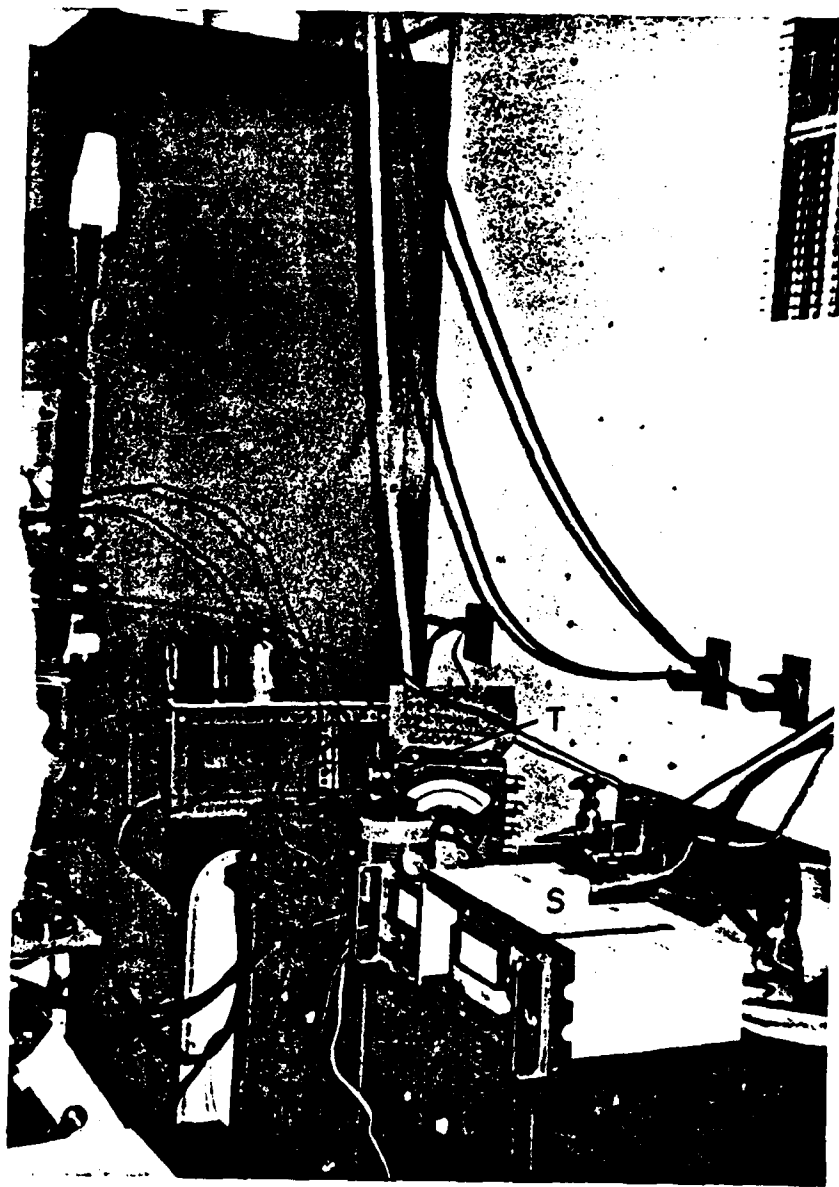


Figure 3B. VUV lamp/monochromator output spectrum obtained with 0.1 torr of ultrahigh purity hydrogen in the discharge lamp. Operating conditions: entrance slit = 0.2 mm. exit slit = 2.0 mm; 7.2×10^{-5} torr (uncorrected) in the monochromator; filament current = 14.9 A AC at 100 V AC; discharge current = 1.5 A DC at 170 V DC. Photomultiplier Voltage = 400 V.

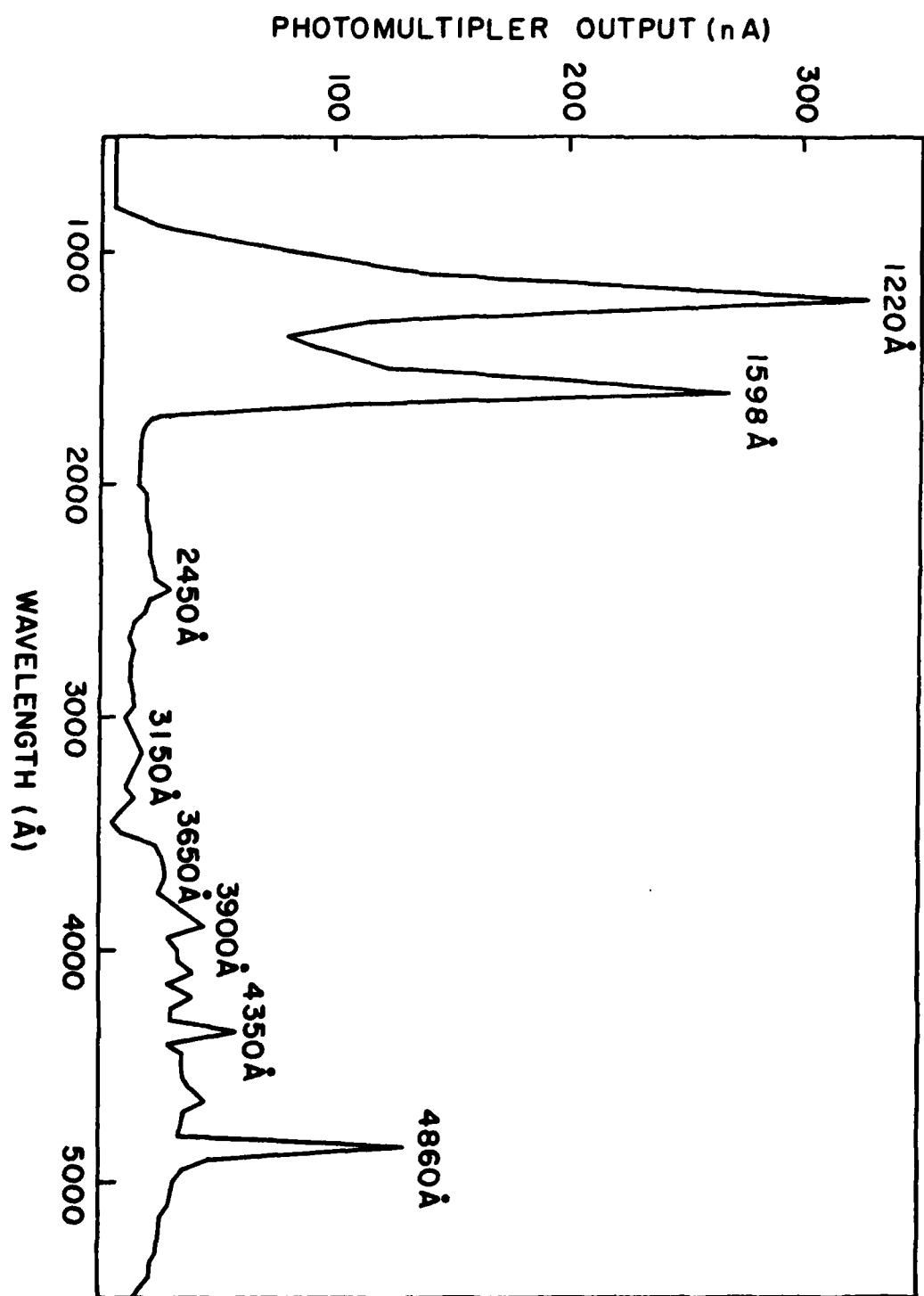
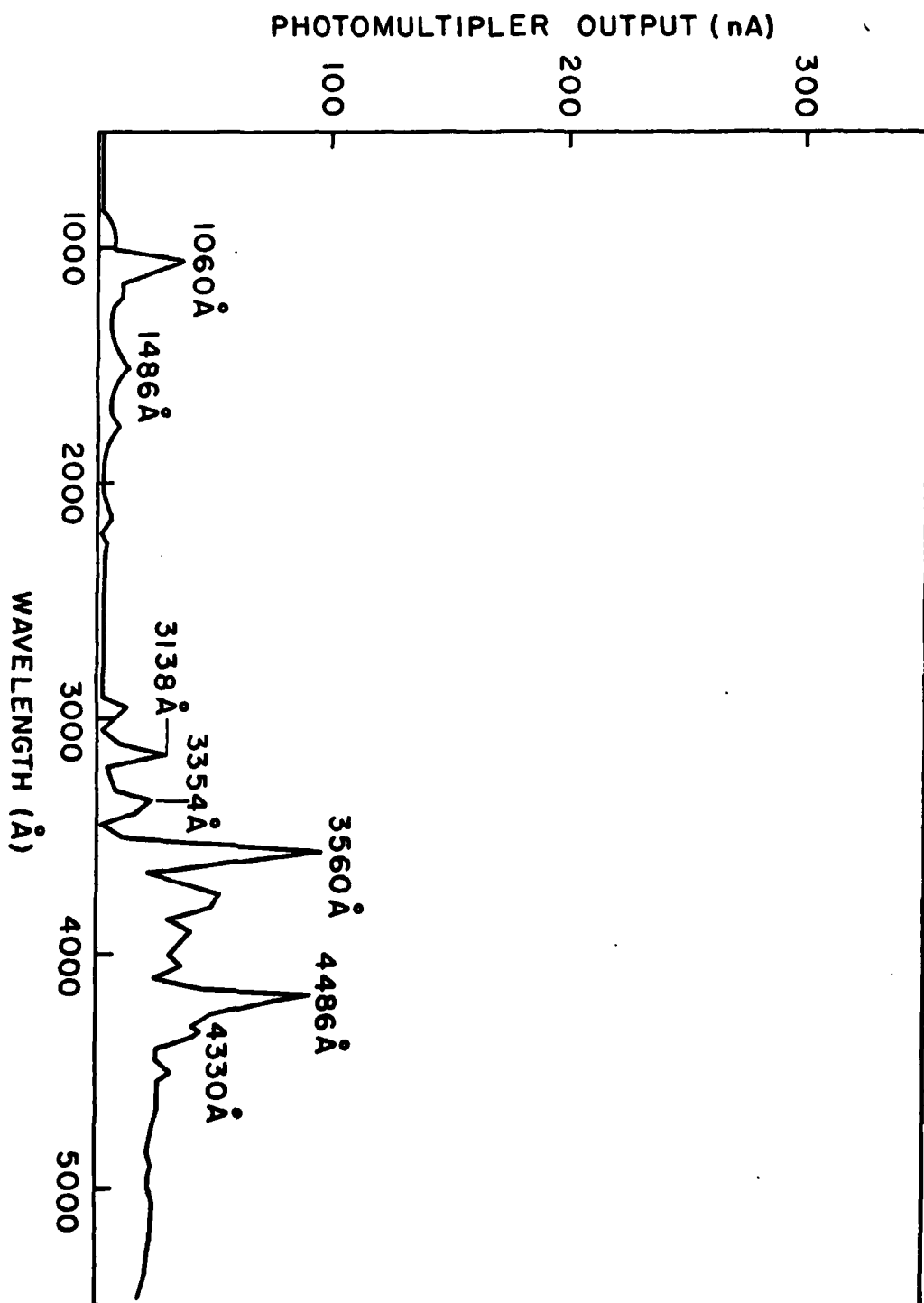


Figure 4B. VUV lamp/monochromator output spectrum obtained with 0.055 torr prepurified argon in the discharge lamp. Operating conditions: entrance slit = 0.2 mm; exit slit = 2.0 mm; 1.5×10^{-4} torr (uncorrected) in the monochromator; filament current 15.0 A AC at 93.5 V AC; discharge current = 1.5 A DC at 135 V DC. Photomultiplier voltage = 400 V.



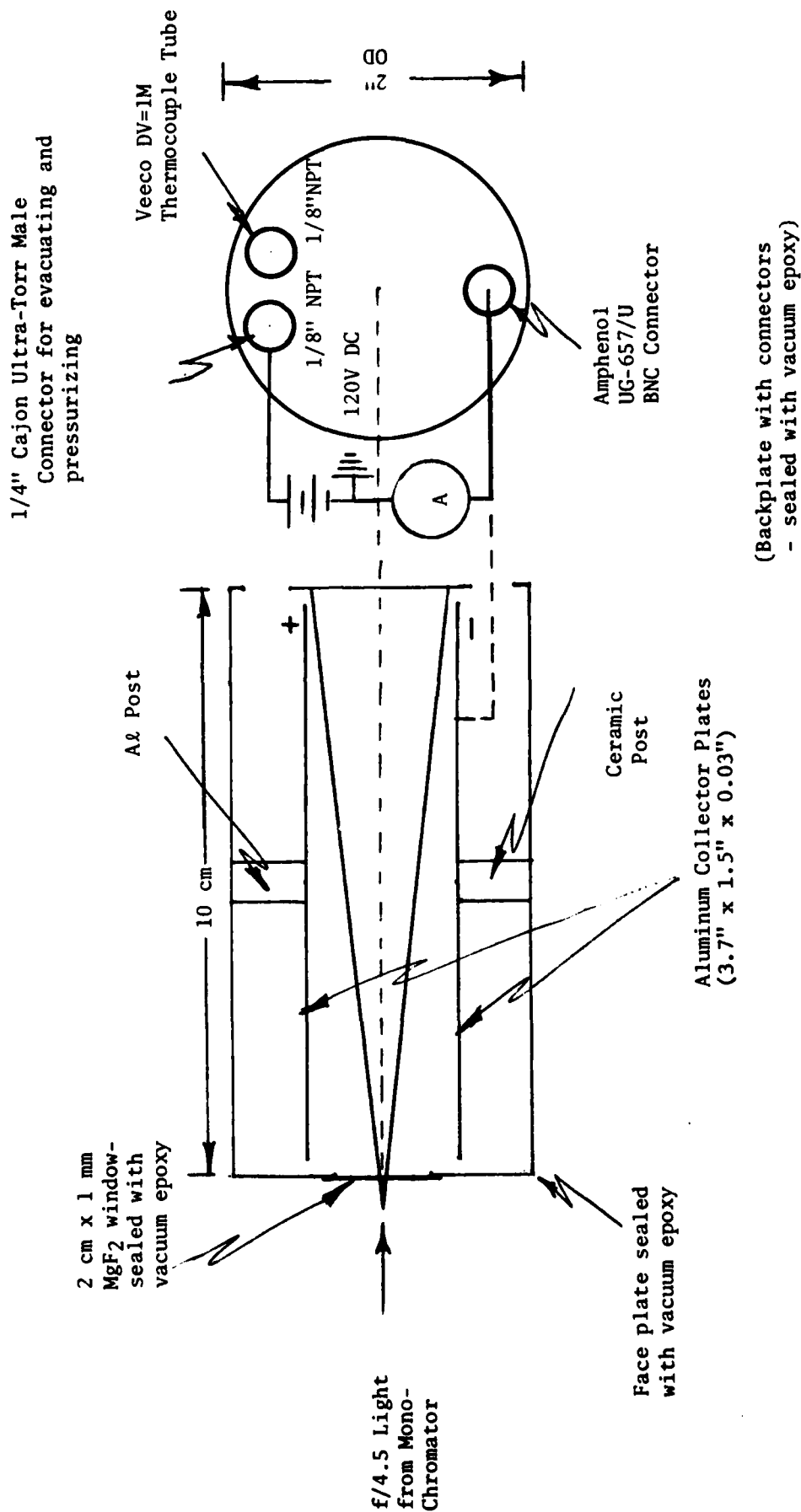
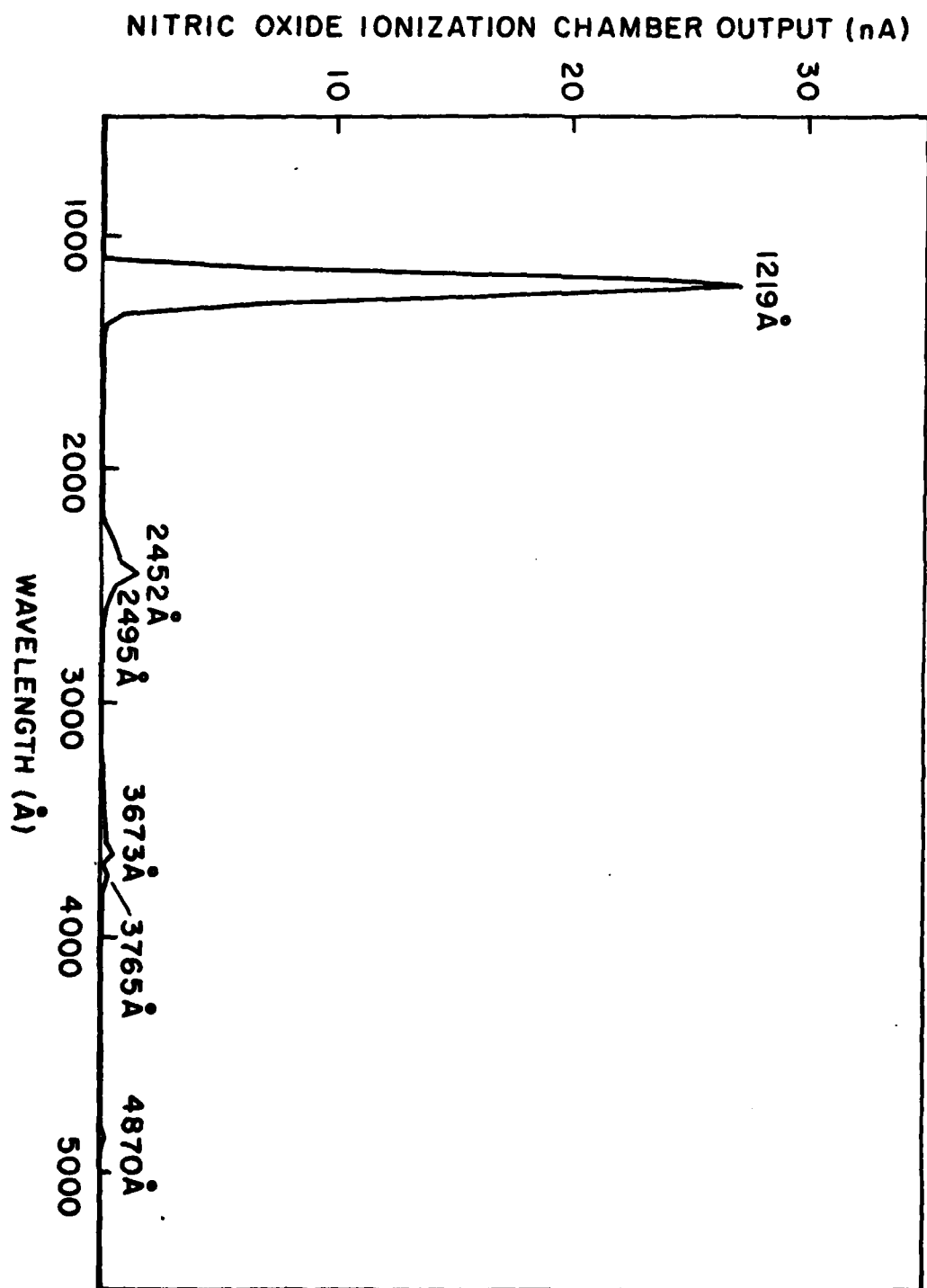


Figure 5B. Schematic of the NO ionization chamber.

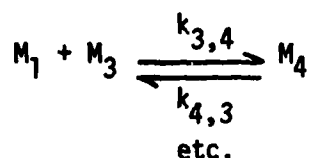
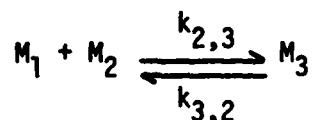
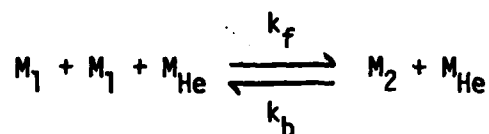
Figure 6B. Collected ion current spectrum in the NO ionization chamber.
Operating conditions: (1) Light source: $P_{H_2} = 0.1$ torr;
entrance slit = 0.2 mm, exit slit = 2.0 mm; 8.9×10^{-5} torr
(uncorrected) in the monochromator; filament current = 13.6 A
AC at 100 VAC; discharge current = 1.5 A DC at 180 VDC;
(2) Ionization chamber: $P_{NO} = 2.04$ torr; 120 VDC collection
potential.



APPENDIX C

Analysis of Cluster Growth Kinetics

Dimer formation is assumed to proceed via a three body mechanism (a third molecule is necessary to carry away the energy of dimerization and to stabilize the collision complex). All subsequent reactions are assumed to proceed via two body reactions. The general reaction sequence is



where M_1 stands for monomer, M_{He} for helium, M_2 for dimer, and so forth.

Cluster-cluster agglomeration reactions are negligible since the monomer concentration is much greater than the cluster population in the early stages of growth.

Neglecting evaporation reactions greatly simplifies the kinetic analysis. The conditions used in this study assure that evaporation reactions can be neglected. This is confirmed by analysis of the equilibrium constant for the reaction $M_1 + M_2 \rightleftharpoons M_3$. Based on bond energies and vibrational and rotational frequencies given by Owicki et. al. (1), an equilibrium constant of $3 \cdot 10^{-11} \text{ cm}^3$ is indicated for this reaction at 100°K. Irreversible growth is assured when

$$[M_1] [M_2] k_{2,3} \gg [M_3] k_{3,2}$$

Assuming $[M_2] \approx [M_3]$, growth will be irreversible for $[M_1] K_{eq} \gg 1$.

Since the monomer density is $\geq 10^{15}/\text{cm}^3$, $K_{\text{eq}}[M_1] \geq 10^4$ @100K.

For pure birth kinetics

$$[\dot{M}_2] = k_f [M_1] [M_1] [M_{\text{He}}] - k_{2,3} [M_1] [M_2]$$

$$[\dot{M}_3] = k_{2,3} [M_1] [M_2] - k_{3,4} [M_1] [M_3]$$

etc.

With initial conditions $[M_2 (t=0)] = [M_2]_0$,

$[M_i (t=0)] = 0 \quad i > 2$, and $[M_1] = [M_1]_0$,

the solution to this set of equations is

$$[M_2(t)] = \frac{k_f [M_1] [M_{\text{He}}]}{k_{2,3}} + \left[[M_2]_0 - \frac{k_f [M_1] [M_{\text{He}}]}{k_{2,3}} \right] e^{-k_{2,3} [M_1] t}$$

$$[M_j(t)] = \frac{k_f [M_1] [M_{\text{He}}]}{k_{j,j+1}} + \left(\prod_{m=2}^{j-1} (-k_{m,m+1}) \right)$$

$$\left[\sum_{n=2}^j c_{m,j} \left([M_2]_0 - \frac{k_f [M_1] [M_{\text{He}}]}{k_{n,n+1}} \right) e^{-k_{n,n+1} [M_1] t} \right]$$

$$\text{where } c_{m,j} = \prod_{\substack{p=2 \\ p \neq n}}^j \left(\frac{1}{k_{n,n+1} - k_{p,p+1}} \right)$$

At long times (but not so long as to deplete the monomer) the cluster concen-

trations reach their steady state value, $\frac{k_f [M_1] [M_{\text{He}}]}{k_{j,j+1}}$. The ratio of steady-state concentrations

gives the relative rate constants, $\frac{[M_{i-1}]^{ss}}{[M_j]^{ss}} = \frac{k_{j,j+1}}{k_{j-1,j}}$. Since the detection system is subject to mass discrimination effects, the measurement of relative rates is obscured by the relative detection efficiency.

The absolute rate constant can be obtained for those clusters where the transient portion of the curve leading to the steady state concentration can be observed. The rate constant is given by

$$k_{j,j+1} = \frac{d[I_j(t)]}{dt} \left\{ \frac{1}{[M_1] \left(\frac{[I_j]^{ss}}{[I_{j-1}]^{ss}} [I_{j-1}(t)] - [I_j(t)] \right)} \right\}$$

where $[I_j(t)]$ is the observed cluster ion signal (2).

All of the quantities on the right hand side can be measured experimentally and the only concentration which needs to be known absolutely is the monomer. The monomer concentration is obtained from the known flow rates into the MECS. Thus, by observing the rise of a cluster signal to its steady state value as the residence time in the growth region is varied, the rate constant for its growth to the next larger cluster by monomer addition can be measured.

If a series of rate constants are determined, then the relative ionization cross sections can be estimated from the ratio of the steady state signals, after correcting for other mass effects.

(1C) Owicki, John C., Shipman, Lester L., and Scheraga, Harold A., J. Phys. Chem., 79, 1794, 1975.

(2C) Kolstad, "Studies of Water Clusters", Ph.D. Thesis, Princeton University, 1982.

DATE
FILMED
— 8